The International Journal of Advanced Manufacturing Technology (2022) 120:1643–1652
https://doi.org/10.1007/s00170-022-08833-w

ORIGINAL ARTICLE

Shielding gas influence on AA5086 welded joints: residual stresses analysis, microstructural characterisation and mechanical properties

Maria Cindra Fonseca[1] · Marcos Caetano Melado[1] · Marcel Freitas de Souza[1] · Cássio Barbosa[2]

Received: 11 October 2021 / Accepted: 26 January 2022 / Published online: 12 February 2022

Abstract

Samples of AA5086 aluminium alloy were welded by gas tungsten arc welding (GTAW) with alternating current using three different shielding gases. The samples were welded with pure argon (Ar), a mixture of argon and helium (Ar + He) and a new mixture composed of argon, nitrous oxide and oxygen ($Ar + N_2O + O_2$). The effect of the shielding gas on the residual stresses and on the mechanical and microstructural properties of the welded joints was evaluated and compared with the base metal. The new gas mixture produced compressive residual stresses in the longitudinal and transverse directions in the weld metal. Tensile test of welded joints indicated similar values for yield strength and ultimate tensile strength; however, these values were lower compared to the base metal. The new gas mixture provided a welded joint with hardness values in the weld metal and heat-affected zone close to the base metal values and with greater magnitude compared to samples welded using pure argon and mixture of argon and helium. Microstructural characterisation performed by optical and scanning electron microscopy showed that the new mixture produced welded joints with lower porosity.

Keywords Aluminium alloy AA5086 · GTAW process · Residual stresses · Mechanical properties · Microstructural characterisation

1 Introduction

Al–Mg alloys (AA 5XXX series) are an important group of non-heat-treatable aluminium alloys that can only be hardened by solid solution and mechanical working. Magnesium is the main alloying element, and additions of up to 6% lead to solute hardening combined with efficient strain hardening. These alloys have a good strength-to-weight ratio, excellent corrosion resistance and good weldability, resulting in a wide range of applications in the marine, chemical and automotive industries [1–5].

The gas tungsten arc welding (GTAW) process provides excellent quality and finishing of welded components and is particularly suitable for the welding of aluminium alloys [6–8]. The shielding gas is used not only to protect the molten drop and bead, but also to modify metal transfer, penetration and bead width of the weld, for spatter control and post-weld cleaning, to control welding fume generation and to influence the metallurgical and mechanical properties of the weld [9].

The shielding gases traditionally used in the welding of aluminium alloys are inert gases, such as pure argon, pure helium or argon/helium blends. Recent researches evaluate shielding gas mixtures for GTAW process with the addition of small amounts of nitrogen, oxygen, and nitrous oxide to increase travel speed, change penetration and reduce surface tension, among other benefits. However, it is necessary to deepen the addition of these gases in traditional shielding gas, since they are more reactive and promote oxidation of the weld metal, especially for aluminium alloys [10]. For these reasons, the choice of shielding gas is a critical factor in the welding process, and numerous researchers have conducted extensive studies and experiments to reduce the overall welding cost and increase the efficiency of the process [11].

Welding residual stresses arise due to differential thermal expansion and contraction of the weld metal and base metal. Although residual stresses are essential for the performance

✉ Maria Cindra Fonseca
mariacindra@id.uff.br

[1] Department of Mechanical Engineering, School of Engineering/PGMEC, Universidade Federal Fluminense, Rua Passo da Patria, 156, Niteroi, RJ 24210-240, Brazil

[2] INT – Instituto Nacional de Tecnologia, Av. Venezuela, 82, Rio de Janeiro, RJ 20081-312, Brazil

Table 1 Chemical composition of AA5086 alloy (% weight)

Si	Fe	Cu	Mn	Mg	Cr	Zn	Ti	Al
0.40	0.50	0.10	0.45	4.00	0.15	0.25	0.15	Balance

and service life of a welded component, there is no specific comparative analysis between different shielding gases used in aluminium alloys welded by GTAW process [11, 12].

Therefore, this work presents innovative research on residual stresses using traditional shielding gas (pure Ar and Ar + He) and also a newly developed mixture of argon with a low concentration of O2 and N2O. Despite the positive results demonstrated for this new mixture, few comprehensive scientific resources are dealing with this issue, which limits its large-scale use on an industrial scale and thus gives the present work a prominent role in better understanding the advantages of new different gas mixtures [11, 12].

The present work aims to study the residual stresses, measured by X-ray diffraction technique using sin2ψ method and mechanical properties (mechanical strength and microhardness) of welded joints by the GTAW process of aluminium alloy AA5086, using different shielding gases. Except shielding gas composition, all other welding parameters were kept constant to determine the output responses. Later, one-way analysis of variance (ANOVA) was done to statically evaluate the significance of shielding gases on the experimental results.

2 Materials and experimental methods

The base metal (BM) used in this work was AA 5086-H116 aluminium alloy manufactured according to ASTM-B 928–04, tempering H-116, in the form of sheet 6.35 mm thick. The chemical composition and nominal mechanical properties of this material are shown in Tables 1 and 2, respectively.

The filler metal was TIG-HARRIS rod, aluminium alloy 5083, with a diameter of 3.2 mm, and its chemical composition is shown in Table 3.

Plates of size 250 × 150 mm, each with one of the edges chamfered by machining, were taken together to form a weld pad of 250 × 300 mm with a single V-groove joint. Figure 1 presents the details of the joint.

The samples were welded by GTAW process (welding machine KEMPPI model Master TIG, 3500 W, AC/DC) using different shielding gas, with alternating current in a flat position, according to the parameters shown in Table 4. For both samples, during the 1st pass (root pass), one locking bar and a back of copper were used to prevent warping of the plates.

Table 2 Mechanical properties of AA5086 alloy

Yield strength — Re (MPa)	Ultimate tensile strength — Rm (MPa)	Hardness (HV)
205	335	88

Residual stresses of the welded samples were measured in the longitudinal (L) and transverse (T) directions to the bead in the weld metal (WM), heat-affected zone (HAZ) and base metal (BM) at the points shown in Fig. 2a. The residual stresses were measured using the Xstress3000 analyser, by X-ray diffraction technique using the sin2ψ method (uncertain of ± 15 MPa), Crκα radiation (λCrκα = 2.29092 Å) and diffracting the (222) plane of aluminium with angle 2θ = 156.98º.

Micrographs of samples of each welding condition were performed. The samples were ground, polished and etched with a solution of 2 ml of HF in 100 ml of water. The etching time was 90 s for WM and HAZ and 60 s for the base metal. The samples were analysed by optical microscopy (OM) and scanning electron microscopy (SEM) with qualitative analysis of porosity in the welded joints.

The Vickers microhardness test was performed with a load of 25 g for 15 s. The measurement of microhardness was carried out at the top, centre and root in the WM, HAZ (left and right of weld bead) and BM (left and right of weld bead). The result for each region is an average of the values obtained at the top, centre and root positions (Fig. 2b).

The tensile test was performed in accordance with ASTM B557M (Fig. 2c) using INSTRON 3382 Testing Machine with a speed of 2 mm/s at room temperature. Four tensile test samples were made for each welding condition and base metal.

One-way ANOVA and Tukey's test were performed with a significance level of 0.05 to evaluate the differences between the values of residual stresses, mechanical properties (Re and Rm) and Vickers microhardness. These analyses are relevant to verify if the use of different shielding gases alters the mechanical properties of welded joints.

3 Results and discussion

Residual stresses in longitudinal and transverse directions were analysed in WM, HAZ and BM in each sample after welding. The results are shown in Fig. 3.

The longitudinal residual stresses (LRSs) at the joints of each welding condition had a homogeneous and tensile behaviour in the HAZ and BM, while the WM showed compressive stresses with the new mixture (Ar + O2 + N2O) and tensile ones with Ar + He and pure Ar. The high longitudinal

Table 3 Chemical composition of AA5083 filler metal (% weight)

Si	Fe	Cu	Mn	Mg	Cr	Zn	Ti	Al
0.40	0.40	0.10	0.70	4.40	0.15	0.25	0.15	Balance

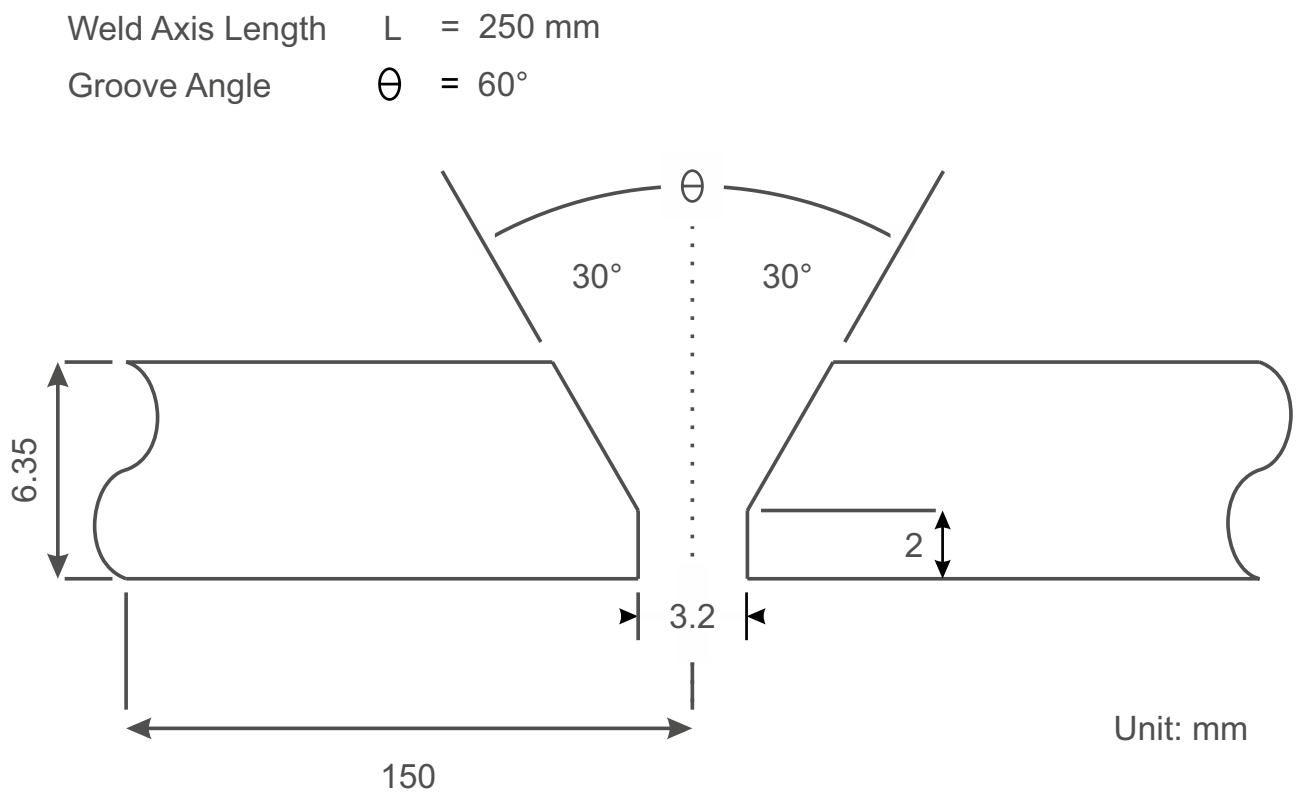

Fig. 1 Welded joint details of single V-groove butt weld

tensile residual stresses in the HAZ may have contributed to the reduction of the mechanical strength of the welded joint, because all specimens broke in this region.

The behaviour of transverse residual stresses (TRS) in welded specimens with the Ar + He and the new gas mixture (Ar + O2 + N2O) was very similar with high compressive values in the BM, low tensile values in the HAZ and compressive in WM. As occurred in the longitudinal direction, the welded joint with the protection of pure Ar can be considered the most critical condition with tensile residual stresses around 50% of the yield strength initially reported by the manufacturer in Table 2.

Therefore, the new mixture showed a beneficial residual stress state in relation to the other welded joints. However, the tensile residual stresses in the HAZ made this region of the joint critical and with a tendency to fail.

The one-way ANOVA was used to determine if there were any statistically significant differences between the means of residual stresses considering the three regions of the joint. The results for a significance level of 0.05 are shown in Table 5.

As the p-values tended to zero for all conditions, it is possible to state that the statistical analysis indicated that there is a significant difference between the means of residual stresses for the three regions when using different shielding gases [13].

Table 6 presents the results of the Tukey test, which was used to compare the difference between each pair of means of residual stresses considering three different shielding gases.

The Tukey test indicated that there is no significant difference between the values of residual stresses in BM and WM in the transverse direction when evaluating the pair Ar + He/Ar + N2O + O2. This result corroborates what is shown in Fig. 3, since both mixtures provided similar residual stresses and more compressive magnitudes compared to the Ar shielding gas. p-value lower than 0.05 indicates that the shielding gases had an obvious effect on residual stresses, and this result was verified in most cases of the comparative analysis [13].

Table 4 Welding parameters

Sample	Shielding Gases	Flow (L/min)	Current (A)	Welding Speed (mm/min)	
				1st Pass (Root)	1st Pass (Root)
1	Ar (pure)	10	202	150	80
2	75% Ar + 25% He	10	202	150	100
3	Ar + 200 ppm of N_2O + 200 pm of O_2	10	202	150	80

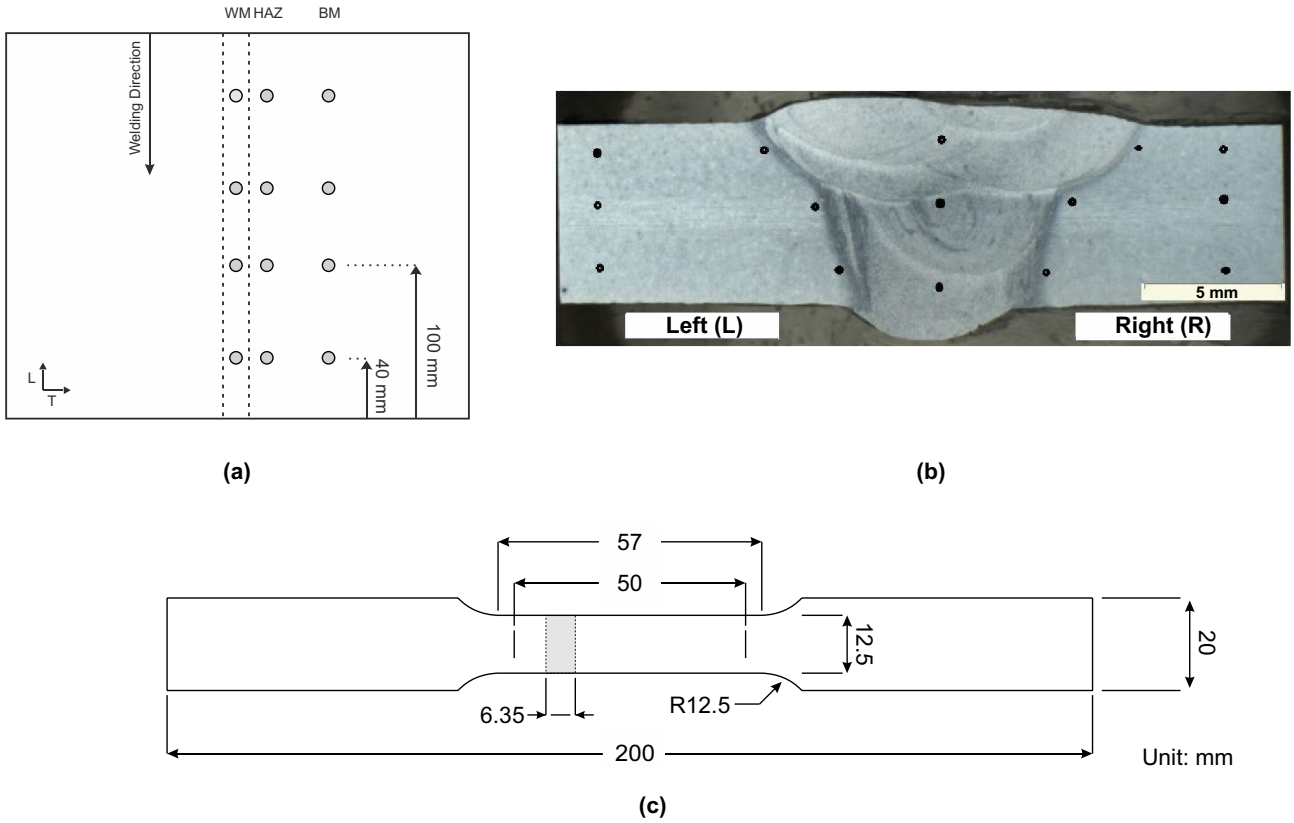

Fig. 2 (**a**) Measurement points of residual stresses; (**b**) measurement points of hardness in the welded joint; (**c**) dimensions of tensile test specimen (ASTM B557M)

Figure 4 shows the presence of pores in WM, especially in welded joints with pure Ar and Ar + He. Porosity is always present in aluminium samples welded by GTAW process with pure Ar, as reported by Prakash et al. [14], and the addition of He to the blend can significantly reduce this defect due to the higher thermal conductivity of He, which results in greater energy transferred to the weld pool.

In Fig. 4c, which corresponds to the welded joint using the new mixture, it can be observed more refined grains and that the formation of porosity was much lower compared to welded joint with previous shielding gases. Additionally, it was verified the presence of a crack, which may have arisen due to the alignment of the pores.

Pores form due to the sharp decrease in hydrogen solubility during the solidification process, since the solubility of hydrogen in molten aluminium is about 20 times higher than in solid aluminium. The formation of pores can be reduced by proper joint preparation, use of high purity shielding gas with low-dew-point and careful storage of the filler metal. However, the 5XXX series filler alloys, as used in this research, are particularly susceptible to surface oxide hydration, which promotes porosity formation [15, 16].

Table 5 Results of one-way ANOVA for residual stresses

Region	LRS		TRS	
	F-value	*p*-value	*F*-value	*p*-value
BM	40	0.000032	114	0
HAZ	164	0	280	0
WM	1234	0	1117	0

In Fig. 5, the joint welded with pure Ar had a more critical porosity profile, with deeper pores compared to joints welded using the other shielding gases, this result being consistent with Prakash et al. [14]. Additionally, Arana et al. [17] also observed that argon generated a greater porosity area percentage compared to a three-phase mixture Ar + O2 + N2O considering the same shielding gas flow rate and deposition strategy in the wire-arc additive manufacturing (WAAM) process with ER5356 filler metal. Figure 5c shows the presence of dispersoids, particles of the Al(Fe)MnSi phase, which inhibit grain growth in aluminium alloys by anchoring the movement of grain boundaries [18, 19].

The joint welded with Ar + He (Fig. 6) presented an intermediate porosity condition, confirming what was noticed in the micrographs by optical microscopy. The pore alignments shown in Fig. 6a can make the joint susceptible to crack formation.

Table 6 Results of Tukey test for residual stresses considering different shielding gases

Shielding gases	*p*-value					
	LRS			TRS		
	BM	HAZ	WM	BM	HAZ	WM
Ar/Ar + He	0.039711	0.000183	0.000183	0.000183	0.000183	0.000183
Ar/Ar + $N_2O + O_2$	0.000197	0.000183	0.000183	0.000183	0.000233	0.000183
Ar + He/Ar + $N_2O + O_2$	0.000763	0.015291	0.000183	1.000000	0.000183	0.356749

Vyskoc et al. [20], evaluating the effect of shielding gases on the properties of AW 5083 aluminium alloy laser-weld joints with 5087 filler metal, found that, compared to the welding process with pure argon, there was a 50% reduction in porosity formation using Ar + 5% He and about 30% using Ar + 30% He. The extra heat potential of He can reduce gas entrapment and thus porosity by widening the weld fusion and penetration in Ar + He blends.

The joint welded with the new mixture (Fig. 7) showed lower porosity, also corroborating what was observed previously by optical microscopy. Although Miller et al. [10] did not perform a specific porosity analysis when using different shielding gases for aluminium alloy welding, the mixture with Ar + 200 ppm N2O + 200 ppm O2 showed an excellent bead appearance and generally better characteristics when compared with the use of only one active gas at the same total concentration.

Figure 8 shows the average values of Re and Rm obtained in the tensile tests carried out on the base metal and for each welding condition.

The welded joints presented, in general, yield strength and ultimate tensile strength equivalent. Vyskoc et al. [20] have shown that the shielding gas does not cause any change in the yield strength and ultimate tensile strength, which can also be seen in Fig. 8. Therefore, it can be concluded from these results that shielding gas was not a significant factor in the tensile mechanical properties.

For all welding conditions, the ultimate tensile strength was about 12% lower compared to the base metal, and the yield strength was reduced by 38% (for samples welded Ar and Ar + He) and 33% (for the sample welded with the new mixture). Srivatsava et al. [21] obtained a yield strength of 150 MPa and ultimate tensile strength of about 290 MPa in samples of AA5083 welded by the non-pulsed GTAW process, being these values lower than those indicated for the base metal. This result is in agreement with Vasu et al. [22] who stated that the tensile properties of welded joints are significantly affected by the loss of alloying elements caused by evaporation.

The weld performed with the new mixture showed better yield strength when compared with other weld joints, especially when compared to the sample welded with Ar, where the difference was 10 MPa. This result was consistent with the microstructural analysis, where the new mixture presented less porous formation and, consequently, less stress concentration. Additionally, the tensile residual

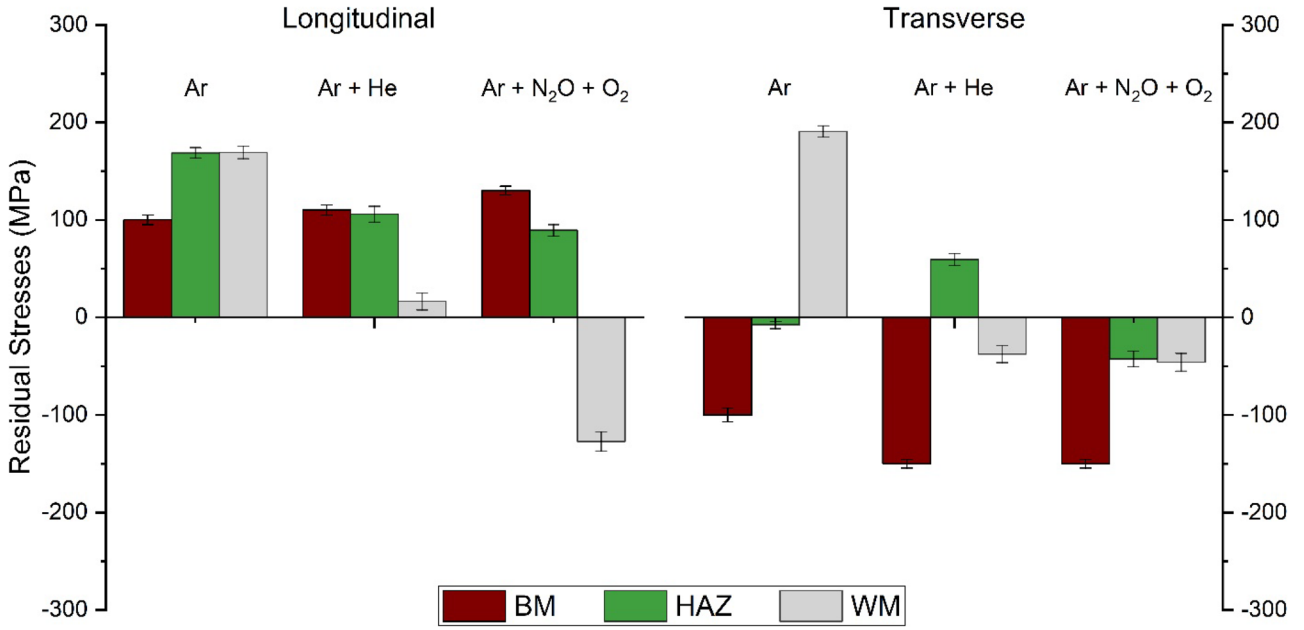

Fig. 3 Residual stresses after welding using different shielding gases

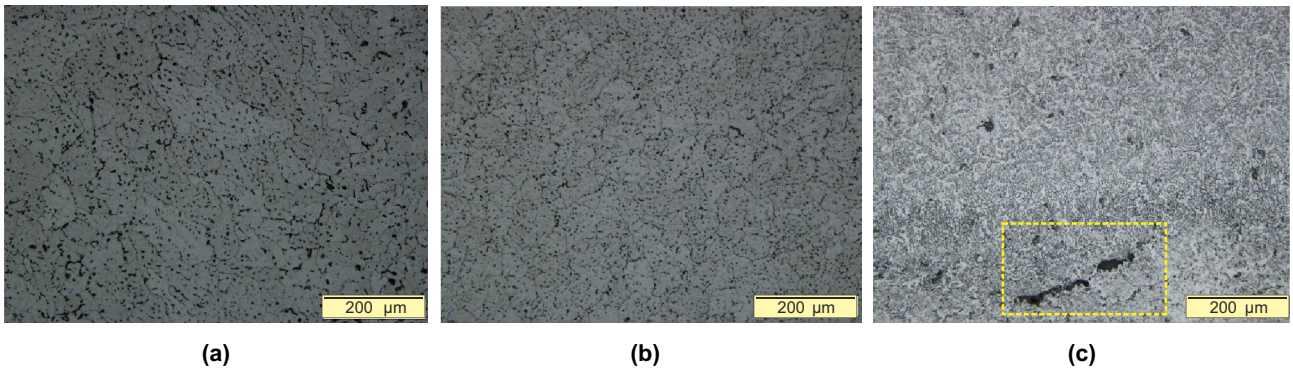

Fig. 4 Optical microscopy of WM using different shielding gases: (**a**) pure Ar; (**b**) Ar + He; (**c**) Ar + N2O + O2 (crack indicated in the yellow rectangle)

stresses in this joint had smaller magnitudes, compared to the other joints, in the longitudinal direction.

In both welding conditions, all specimens fractured in the HAZ, which is consistent with the microstructural analysis, since the grains are coarser in this region, reducing the resistance of the material. The influence of tensile residual stresses in this region may also have occurred.

Table 7 presents the one-way ANOVA test for the mechanical properties.

The p-value tended to zero for both Re and Rm. Therefore, it is possible to state that the statistical analysis indicated that there is a difference between the mean of these properties when using different shielding gases.

Table 8 presents the results of the Tukey test.

The Tukey test indicated a significant difference in mechanical properties results when comparing the BM and welded joints with the three shielding gases, as shown in Fig. 8 with a considerable reduction of Re and Rm. However, except for the Re of the Ar/Ar + N2O + O2 pair, it was verified that there is no significant difference in the mechanical properties of the welded joints.

Vickers microhardness results are presented in Fig. 9.

The Vickers microhardness of the samples welded with Ar and Ar + He was similar. The BM presented a higher value in relation to the HAZ and WM in both conditions.

Vasu et al. [22] also observed higher hardness values in the BM compared to the WM in AA5059-H136 aluminium alloy–welded joints by GTAW and GMAW processes.

Vyskoc et al. [20] also found that the lowest Vickers microhardness values in the weld bead were obtained when welding with Ar and, thus, the use of He in the mixture caused an increase in this mechanical property. They reported that the Vickers microhardness in the centre of the weld bead was 59 HV for Ar and 60 HV for Ar + 30% He, and these values are close to those observed in Fig. 9.

The new mixture (Ar + N2O + O2) provided a joint with average microhardness values in HAZ and WM close to BM and with greater magnitude in relation to the other welded joints. These results of the new mixture are consistent with the microstructure analysis, which showed refined grains in the WM.

Table 9 presents the one-way ANOVA test result for the Vickers microhardness.

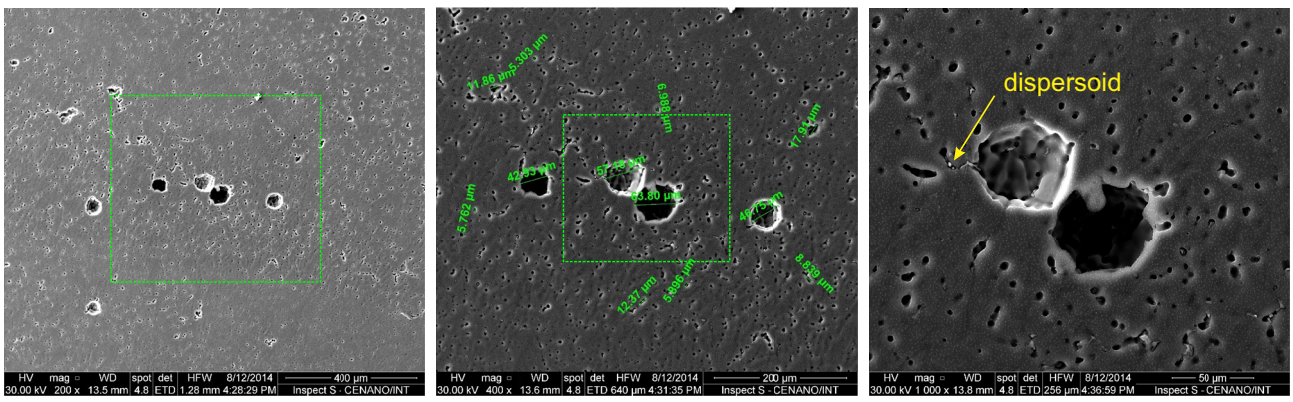

Fig. 5 SEM of the welded joint with pure argon protection: (**a**) high porous concentration, (**b**) magnification of the area indicated in (**a**), (**c**) magnification of the area indicated in (**b**)

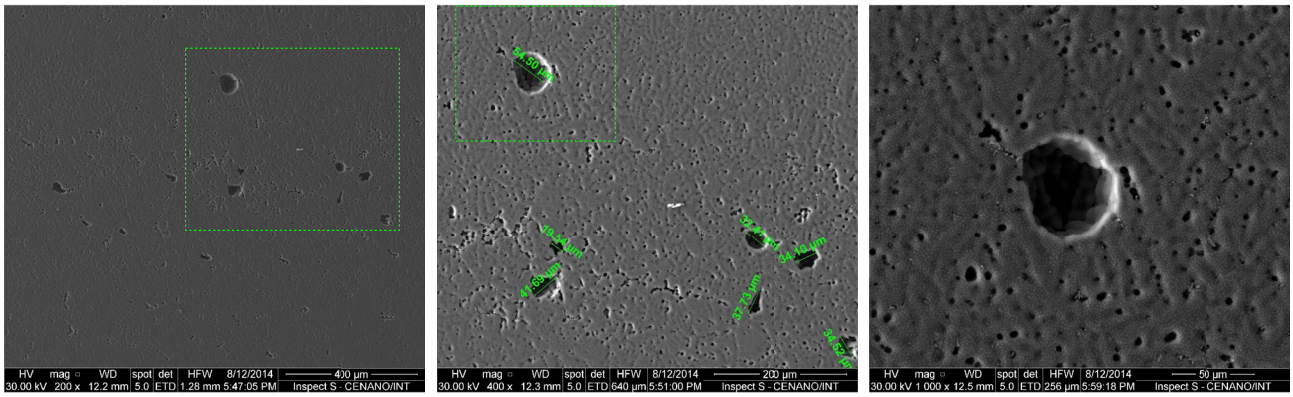

Fig. 6 SEM of the welded joint with a mixture of Ar + He: (**a**) intermediate porous concentration, (**b**) magnification of the area indicated in (**a**), (**c**) magnification of the area indicated in (**b**)

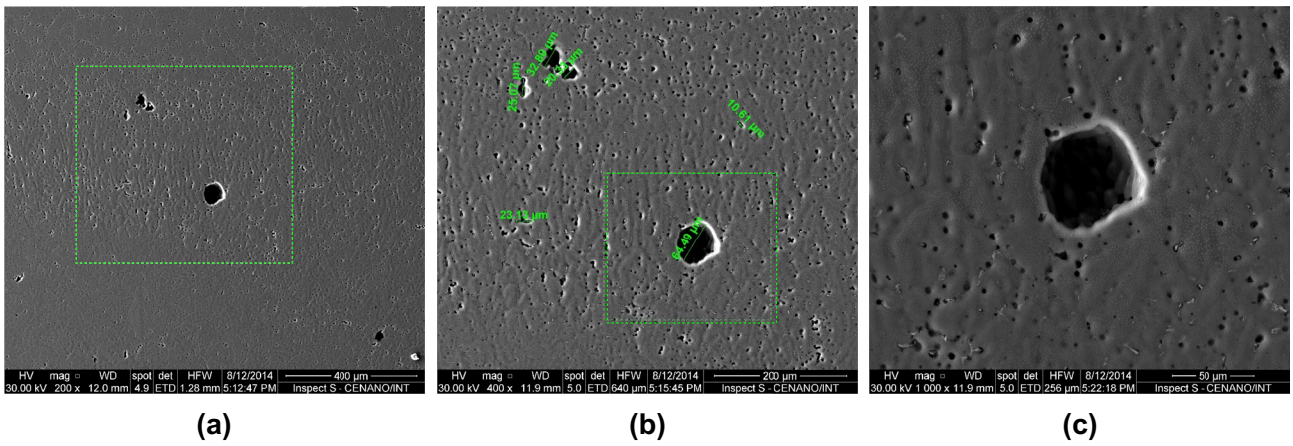

Fig. 7 SEM of the welded joint with the new mixture (Ar + O2 + N2O): (**a**) low porous concentration, (**b**) amplification of the area indicated in (**a**), (**c**) amplification of the area indicated in (**b**)

Table 7 Results of one-way ANOVA for mechanical properties

Re		Rm	
F-value	*p*-value	*F*-value	*p*-value
527	0	137	0

Table 8 Results of Tukey test for mechanical properties

Shielding gases	*p*-value	
	Re	Rm
BM/Ar	0.000199	0.000199
BM/Ar + He	0.000199	0.000199
BM/Ar + $N_2O + O_2$	0.000199	0.000199
Ar/Ar + He	0.352428	0.343118
Ar/Ar + $N_2O + O_2$	0.006325	0.302953
Ar + He/Ar + $N_2O + O_2$	0.122156	0.999728

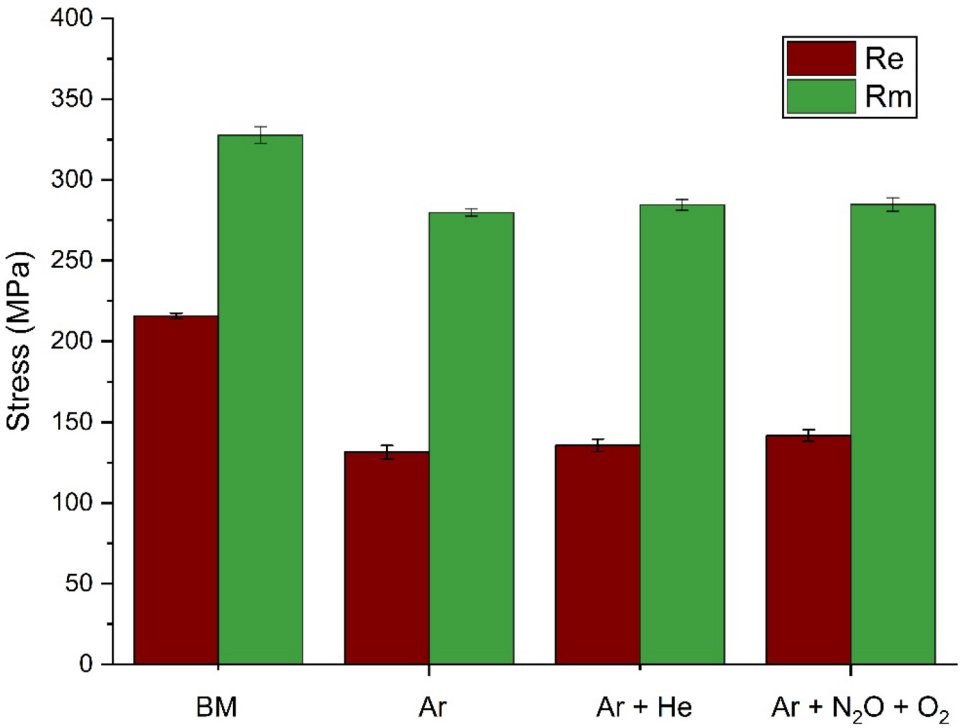

Fig. 8 Mechanical properties of welded joints

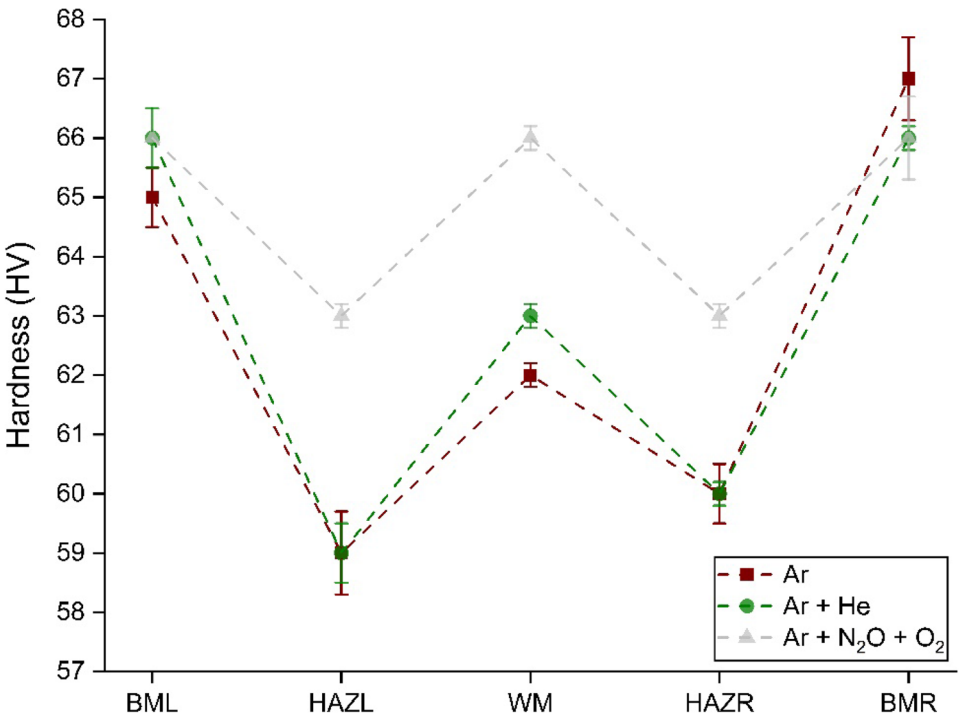

Fig. 9 Vickers microhardness in welded joints

Table 9 Results of one-way ANOVA for Vickers microhardness

Region	*F*-value	*p*-value
BML	1.62	0.272916
HAZL	8.17	0.019391
WM	26.3	0.001070
HAZR	17.17	0.003292
BMR	0.90	0.453503

Table 10 Results of Tukey test for Vickers microhardness

Shielding gases	*p*-value				
	BM	HAZ	WM	HAZ	BM
Ar/Ar + He	0.445995	1	0.165591	0.603569	0.428094
Ar/Ar + $N_2O + O_2$	0.269498	0.029823	0.001161	0.003803	0.715799
Ar + He/Ar + $N_2O + O_2$	0.903494	0.029823	0.006325	0.009905	0.857861

The one-way ANOVA indicated that there is no significant difference between the Vickers microhardness means of BM. However, there is a significant difference between HAZ and WM, which makes it necessary to perform the Tukey test, shown in Table 10.

The statistical difference related to the p-value of the one-way ANOVA test for HAZ and WM in Table 9 is due to the higher Vickers microhardness value when using Ar+N2O+O2, because the p-value was lower than 0.05 in Table 10.

4 Conclusions

The present work, which aimed to study the residual stresses and mechanical properties of welded joints by the GTAW process of aluminium alloy AA5086, using different shielding gases, allowed the following conclusions:

1. The gas mixtures of argon with helium and the new mixture (Ar + 200 ppm N_2O + 200 ppm O_2) provided welded joints with a better residual stress state in the WM compared to pure argon shielding gas.
2. Microstructural analysis showed the presence of porosity in the WM in all joints. However, the new mixture provided less porosity and more refined grains in the WM and HAZ, thus enabling better mechanical properties.
3. The welded joints showed similar yield strength and ultimate tensile strength, but these values were lower than those of the base metal. The joint welded with the new mixture presented a small improvement in mechanical properties compared to the other joints.
4. The new mixture provided a welded joint with hardness values in the WM and HAZ to the BM values and with greater magnitude compared to samples using traditional shielding gases (pure Ar and Ar + He).

Author contribution Maria Cindra Fonseca: Conceptualization, Formal analysis, Funding acquisition, Investigation, Methodology, Project administration, Resources, Supervision, Validation, Visualization, Writing — review and editing. Marcos Caetano Melado: conceptualization, formal analysis, investigation, methodology, writing — original draft. Marcel Freitas de Souza: investigation, writing — original draft, writing — review and editing. Cássio Barbosa: investigation, methodology, resources, supervision, validation, writing — original draft.

Funding This study was financed in part by the Coordenação de Aperfeiçoamento de Pessoal de Nível Superior—Brasil (CAPES)—Finance Code 001. White Martins Company the welded sample and the Brazilian research agencies CNPq (304129/2018–6) and FAPERJ provided financial support.

Declarations

Ethics approval Not applicable.

Consent to participate Written informed consent for publication was obtained from all participants.

Consent for publication Written informed consent for publication was obtained from all participants.

Conflict of interest The authors declare no competing interests.

References

1. Wang BB, Xue P, Xiao BL, Wang WG (2020) Achieving equal fatigue strength to base material in a friction stir welded 5083–H19 aluminium alloy joint. Sci Technol Weld Joining 20:81–88. https://doi.org/10.1080/13621718.2019.1630571
2. Babu N, Natarajan U, Malayalamurthi R (2020) Evaluating mechanical and metallurgical properties of gas tungsten arc welded AA 5059 aluminium alloy joints. Mater Today Proc 22:353–363. https://doi.org/10.1016/j.matpr.2019.06.696
3. Engler O, Kuhnke K, Hasenclever J (2017) Development of intermetallic particles during solidification and homogenization of two AA 5xxx series Al-Mg alloys with different Mg contents. J Alloys Compd 728:669–681. https://doi.org/10.1016/j.jallcom.2017.09.060
4. Foley DL, Leff AC, Lang AC, Taheri ML (2020) Evolution of β-phase precipitates in an aluminum-magnesium alloy at the nanoscale. Acta Mater 185:279–286. https://doi.org/10.1016/j.actamat.2019.10.024
5. Fillizzola DM, Santos TS, Miranda AG et al (2021) Annealing effect on the microstructure and mechanical properties of AA 5182 aluminum alloy. Mater Res 24(4):e20200545. https://doi.org/10.1590/1980-5373-MR-2020-0545
6. Venkat Ramana G, Yelamasetti B, Vishnu Vardhan T (2021) Study on weldability and effect of post heat treatment on mechanical and metallurgical properties of dissimilar AA 2025, AA 5083 and AA7075 GTAW weld joints. Mater Today Proc 46:878–882. https://doi.org/10.1016/j.matpr.2020.12.1115
7. Sathishkumar D, Das AD (2021) Investigations on effect of process parameters on GTAW of aluminium alloy welding using full factorial design technique. Mater Today Proc 37:621–626. https://doi.org/10.1016/j.matpr.2020.05.624
8. Zhang Z, Zhang L, Wen G (2019) Study of inner porosity detection for Al-Mg alloy in arc welding through online optical spectroscopy: correlation and feature reduction. J Manuf Processes 39:79–92. https://doi.org/10.1016/j.jmapro.2019.02.016
9. Mvola B, Kah P (2017) Effects of shielding gas control: welded joint properties in GMAW process optimization. Int J Adv Manuf Technol 88:2369–2387. https://doi.org/10.1007/s00170-016-8936-2
10. Miller PL, Lyttle KA, Neff JB et al (2021) Praxair Technology, assignee. Welding gas compositions and method for use. United States patent US 11:040-417 B2
11. Kah P, Martikainen J (2013) Influence of shielding gases in the welding of metals. Int J Adv Manuf Technol 64:1411–1421. https://doi.org/10.1007/s00170-012-4111-6
12. Wan Q, Zhao Y, Zhao T, Yan D, Wang G, Wu A (2021) Influence of restraint conditions on residual stress and distortion of 2219–T8 aluminum alloy TIG welded joints based on contour method. J Manuf Processes 68:796–806. https://doi.org/10.1016/j.jmapro.2021.05.065
13. Wang J, Wang X, Wang Y, Wang M (2021) Effects of forming parameters on fatigue life in incremental sheet punching. Materials 14:2308. https://doi.org/10.3390/ma14092308

14. Prakash J, Tewari SP, Srivastava BK (2011) Shielding gas for welding of aluminium alloys by TIG/MIG welding-a review. Int J Mod Eng Res 1:690–699
15. Hakem M, Lebaili S, Miroud J, Bentaleb A, Toukali S (2012) Welding and characterization of 5083 aluminium alloy. Metal 23:1–6
16. Poolperm P, Nakkiew W, Naksuk N (2020) Finite element analysis of the effect of porosity on residual stress in 2024 aluminium alloy GTAW. Mater Res Express 7:056518. https://doi.org/10.1088/2053-1591/ab906a
17. Arana M, Ukar E, Rodriguez I, Iturrioz A, Alvarez P (2021) Strategies to reduce porosity in Al-MgWAAM parts and their impact on mechanical properties. Metals 11:524. https://doi.org/10.3390/met11030524
18. Saimoto S, Singh MA, Langille MR, Kula A, Niewczas (2018) Identification of the role of Al-Fe-Mn-Si large casting dispersoids in age-hardenable aluminum alloys using small angle X-ray scattering. Mat Sci Eng A 734:51–58. https://doi.org/10.1016/j.msea.2018.07.085
19. Pan S, Quian F, Li C, Wang Z, Li Y (2021) Synergistic strengthening by nano-sized α-Al(Mn, Fe)Si and Al3Zr dispersoids in a heat-resistant Al–Mn–Fe–Si–Zr alloy. Mat Sci Eng A 819:141460. https://doi.org/10.1016/j.msea.2021.141460
20. Vyskoc M, Sahul M, Sahul M (2018) Effect of shielding gas on the properties of AW 5083 aluminum alloy laser weld joints. J Mater Eng Perform 27:2993–3006. https://doi.org/10.1007/s11665-018-3383-x
21. Srivatsava M, Vang G, Kumar GNS (2016) Experimental study of mechanical properties of 5083 aluminium alloy using gas tungsten arc welding. Int J Innov Res Sci Eng Technol 6:7324:7331. https://doi.org/10.15680/IJIRSET.2016.0505098
22. Vasu K, Chelladurai H, Ramaswamy A, Malarvizhi S, Balasubramanian V (2019) Effect of fusion welding processes on tensile properties of armor grade, high thickness, non-heat treatable aluminium alloy joints. Def Technol 15(3):353:362. https://doi.org/10.1016/j.dt.2018.11.004